

Thermal growth of silicon oxynitride films on Si: A reaction-diffusion approach

R. M. C. de Almeida, I. J. R. Baumvol, J. J. Ganem, I. Trimaille, and S. Rigo

Citation: [Journal of Applied Physics](#) **95**, 1770 (2004); doi: 10.1063/1.1639139

View online: <http://dx.doi.org/10.1063/1.1639139>

View Table of Contents: <http://scitation.aip.org/content/aip/journal/jap/95/4?ver=pdfcov>

Published by the [AIP Publishing](#)



Re-register for Table of Content Alerts

Create a profile.



Sign up today!



Thermal growth of silicon oxynitride films on Si: A reaction-diffusion approach

R. M. C. de Almeida^{a)}

Instituto de Física, Universidade Federal do Rio Grande do Sul C. P. 15051, 91501-970 Porto Alegre, RS, Brazil

I. J. R. Baumvol

Centro de Ciências Exatas e Tecnológicas, Universidade de Caxias do Sul 95570-060 Caxias do Sul, RS, Brazil

J. J. Ganem, I. Trimaille, and S. Rigo

Groupe de Physique des Solides, Universités de Paris 6 et 7, UMR 7558 du CNRS, 2 Place Jussieu, 75251, Paris, France

(Received 17 June 2003; accepted 17 November 2003)

We present some experimental results and propose a reaction-diffusion model to describe thermal growth of silicon oxynitride films on Si in NO and N₂O, as well as annealing in NO of thermally grown silicon oxide films on Si. We obtain growth kinetics and N and O depth distributions for the different growth routes by changing only initial and boundary conditions of a set of nonlinear differential equations. The results suggest that the puzzling differences in film growth rate and N incorporation originate from dynamical effects, rather than in differences in chemical reactions. © 2004 American Institute of Physics. [DOI: 10.1063/1.1639139]

I. INTRODUCTION

Electron tunneling through ultrathin gate dielectric layers is currently inhibiting the so far outstanding evolution of the silicon age.¹ While the use of alternative high-*k* dielectric materials to SiO₂ (Refs. 2 and 3) is not introduced in fabrication technology, silicon oxynitride ultrathin films is the interim solution as a dielectric material to produce advanced, ultralarge scale integrated, silicon-based, metal-oxide-semiconductor field-effect transistors.⁴ Using silicon oxynitrides as a replacement for SiO₂ (dielectric constants: $k_{\text{Si}_3\text{N}_4} = 7.9$, $k_{\text{SiO}_2} = 3.9$), it is possible to reduce electron tunneling by simply increasing the physical thickness of the gate dielectric, without decreasing its capacitance.³ Also, the oxynitride/silicon interface is more resistant to dielectric degradation caused by hot electron irradiation and N addition to SiO₂ generates a much better barrier to B diffusion than pure SiO₂.^{4,5} Furthermore, research in the area of high-*k* dielectrics on Si points out the need of an intermediate ultrathin silicon oxynitride layer between the high-*k* dielectric and the active region of the Si semiconductor in order to preserve the electrical advantages of the SiO₂/Si interface.

Different routes are usually followed for the thermal growth of silicon oxynitride films on Si, such as bare silicon in NO or N₂O atmospheres or annealing in NO of thermally grown silicon oxide films on Si.^{4,6} To the best of our knowledge, there is no model that describes the unique features involved in the growth kinetics, composition, and depth distribution of the species, although some theoretical results for growth kinetics only and in the specific route of annealing in NO of silicon oxide films on Si have recently appeared in the

literature. The latter assume abrupt interfaces and stationary NO diffusion through the silicon oxide film.⁷ Thermal growth of silicon oxynitride films on Si has many complicating features in comparison to the oxide film case:⁸ (i) There are various diffusing species, like NO, O₂, N, and O;⁹ (ii) several different chemical reactions take place in the bulk, surface, and interface of the growing SiO_{*x*}N_{*y*} films;¹⁰ (iii) N incorporation creates a diffusion barrier to all diffusing species, the barrier efficiency increasing with N concentration,¹¹ such that N concentration dependent diffusivities must be taken into account; and (iv) further aspects are faster growth kinetics in N₂O as compared to NO, and the fact that incorporated N piles up in the SiO_{*x*}N_{*y*}/Si near-interface region.⁴ This article investigates the growth kinetics and N depth distribution in silicon oxynitride films thermally grown on Si in the three routes mentioned above. Experimental results are reported and a model is presented which is capable of describing the peculiar features of silicon oxynitride growth. This constitutes essential knowledge for integrated circuit simulation and design as well as for fabrication routines.

Typical O and N incorporation kinetics and N profiles are presented in Fig. 1. Areal densities of O and N in the films were determined by means of nuclear reaction analysis.⁹ Oxynitride film thickness can be estimated from O and N areal densities using the nominal mass densities of SiO₂ and Si₃N₄ and Bragg's rule. Growth in N₂O leads to much faster kinetics than in NO and to a much smaller N incorporation. Growth rates are also different for direct growth in NO as compared to nitridation of a SiO₂ film in NO. N profiles were determined in characteristic points of the kinetics curves with a depth resolution of approximately 0.7 nm. The method consisted of performing rapid thermal growth in ¹⁵N-enriched NO and N₂O (¹⁵NO and ¹⁵N₂O) gases and using narrow nuclear reaction resonance profiling⁹

^{a)}Electronic mail: rita@if.ufrgs.br

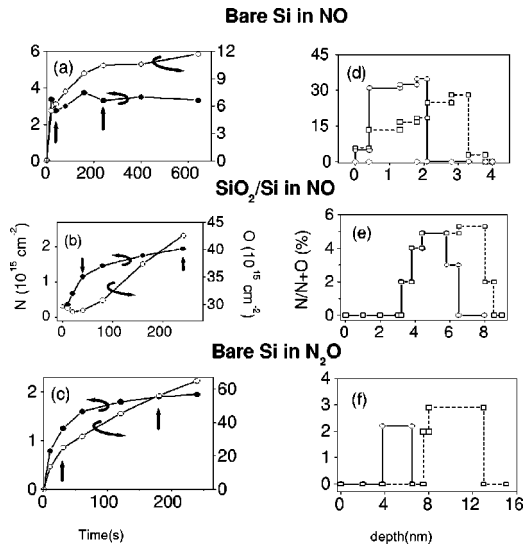
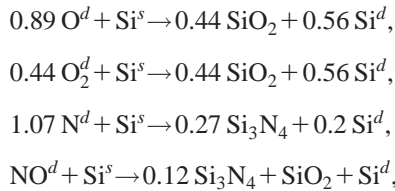


FIG. 1. (Left-hand side) Areal densities of O and N incorporated in silicon oxynitride films rapid thermally grown on Si in NO, N₂O, and in annealing of thermal SiO₂ films on Si in NO. Growth temperature was 1050 °C and gas pressure 30 mbar. (Right-hand side) N profiles for some points, indicated by vertical arrows, of the kinetics curves on the left-hand side.

by means of the resonance at 429 keV in the ¹⁵N(*p*, γ)¹⁶O nuclear reaction. Nitrogen is incorporated mainly in near-interface regions with a nitrogen front following the interface.

II. MODEL

Growth of silicon oxide and oxynitride films on Si is modeled by considering bulk silicon concentration function ρ_{Si}(*x*, *t*) where *x* > 0 is the direction perpendicular to the sample surface, at *x* = 0. When exposed to NO and/or O₂ at high temperatures, the following chemical reactions take place: (i) The surface may catalyze NO and O₂ dissociation. Nondissociated NO and O₂, as well as N and O, constitute diffusive species⁴ with concentrations ρ_{*i*}(*x*, *t*), with *i* = NO, O₂, N, and O, respectively, all normalized with respect to silicon bulk concentration. (ii) Atomic nitrogen and oxygen may recombine, generating N₂ and O₂. Molecular nitrogen is inert and hence will not be explicitly considered. (iii) Diffusive species may either oxidize, nitride, or oxynitride Si, fixing N and O. Mobile silicon may eventually be produced as Si interstitials or SiO. One assumes the following chemical reactions:



where *d* stands for diffusive and *s* for substrate. Volume conservation has been explicitly considered in this set of equations, taking into account the number of Si atoms per unit volume in crystalline-Si, SiO₂, and Si₃N₄ as, respectively, 5, 2.22, and 4 in units of 10²² Si/cm³, yielding fractional stoichiometric coefficients. For example, in the same

volume occupied by a mole of silicon atoms in bulk, after nitridation only 4/5 mole will rest, representing 4/15 = 0.27 mole of Si₃N₄, and requiring 16/15 = 1.07 mole of N atoms while producing 1/5 = 0.2 mole of diffusive Si atoms. The fourth equation above assumes that, in the reaction between NO and substrate-Si, N and O atoms are incorporated at the same rate.¹² (iv) N profile time evolution¹² is taken as a consequence of fixed nitrogen displacement by diffusive oxygen:¹³



These reactions also imply that some silicon is rendered mobile and we emphasize that precise stoichiometric coefficients must still be appropriately determined. Reaction-diffusion equations^{8,14} can then be written. Boundary conditions at the surface (*x* = 0), considering O₂ and NO partial pressures as, respectively, *P*_{O₂} and *P*_{NO}, together with dissociation and the consequent O and N production are written as: ρ_{NO}(0, *t*) = *P*_{NO} - *k*₁*P*_{NO}, ρ_{O₂}(0, *t*) = *P*_{O₂} - *k*₂*P*_{O₂}, ρ_N(0, *t*) = *k*₁*P*_{NO}, ρ_O(0, *t*) = *k*₁*P*_{NO} + 2*k*₂*P*_{O₂}. The local concentrations obey the following equations for *x* > 0:

$$\begin{aligned}
 \frac{\partial \rho_{\text{NO}}}{\partial t} &= D_{\text{NO}} \frac{\partial^2 \rho_{\text{NO}}}{\partial x^2} - \rho_{\text{NO}} \frac{\partial^2 D_{\text{NO}}}{\partial x^2} - 0.48 k_3 \rho_{\text{NO}} \rho_{\text{Si}}^{\text{nr}} \\
 \frac{\partial \rho_{\text{O}}}{\partial t} &= D_{\text{O}} \frac{\partial^2 \rho_{\text{O}}}{\partial x^2} - \rho_{\text{O}} \frac{\partial^2 D_{\text{O}}}{\partial x^2} - 2 k_4 \rho_{\text{O}}^2 - 1.11 k_5 \rho_{\text{O}} \rho_{\text{N}}^f \\
 &\quad - 0.89 k_6 \rho_{\text{O}} \rho_{\text{Si}}^{\text{nr}}, \\
 \frac{\partial \rho_{\text{O}_2}}{\partial t} &= D_{\text{O}_2} \frac{\partial^2 \rho_{\text{O}_2}}{\partial x^2} - \rho_{\text{O}_2} \frac{\partial^2 D_{\text{O}_2}}{\partial x^2} + k_4 \rho_{\text{O}}^2 - 0.44 k_7 \rho_{\text{O}_2} \rho_{\text{Si}}^{\text{nr}}, \\
 \frac{\partial \rho_{\text{N}}}{\partial t} &= D_{\text{N}} \frac{\partial^2 \rho_{\text{N}}}{\partial x^2} - \rho_{\text{N}} \frac{\partial^2 D_{\text{N}}}{\partial x^2} - 2 k_8 \rho_{\text{N}}^2 - 1.33 k_5 \rho_{\text{O}} \rho_{\text{N}}^f \\
 &\quad - 1.07 k_9 \rho_{\text{N}} \rho_{\text{Si}}^{\text{nr}}, \\
 \frac{\partial \rho_{\text{N}^f}}{\partial t} &= 0.36 k_3 \rho_{\text{NO}} \rho_{\text{Si}}^{\text{nr}} - 1.33 k_5 \rho_{\text{O}} \rho_{\text{N}^f} + 1.07 k_9 \rho_{\text{N}} \rho_{\text{Si}}^{\text{nr}}, \\
 \frac{\partial \rho_{\text{O}^f}}{\partial t} &= 0.48 k_3 \rho_{\text{NO}} \rho_{\text{Si}}^{\text{nr}} + 1.11 k_5 \rho_{\text{O}} \rho_{\text{N}^f} + 0.89 k_6 \rho_{\text{O}} \rho_{\text{Si}}^{\text{nr}} \\
 &\quad + 0.89 k_7 \rho_{\text{O}_2} \rho_{\text{Si}}^{\text{nr}}, \\
 \frac{\partial \rho_{\text{Si}}}{\partial t} &= -0.39 k_3 \rho_{\text{NO}} \rho_{\text{Si}}^{\text{nr}} - 0.44 k_5 \rho_{\text{O}} \rho_{\text{N}^f} - 0.56 k_6 \rho_{\text{O}} \rho_{\text{Si}}^{\text{nr}} \\
 &\quad - 0.56 k_7 \rho_{\text{O}_2} \rho_{\text{Si}}^{\text{nr}} - 0.2 k_9 \rho_{\text{N}} \rho_{\text{Si}}^{\text{nr}},
 \end{aligned} \tag{1}$$

where the superscript *f* stands for fixed species and ρ_{Si}^{nr} for the concentration of Si atoms that have not yet fully reacted with oxygen or nitrogen, that is, ρ_{Si}^{nr} = ρ_{Si} - 4/3 ρ_{N^f} - 1/2 ρ_{O^f}, such that ρ_{Si}^{nr} = 0 in (i) the pure oxide (SiO₂), (ii) the pure nitride (Si₃N₄), or (iii) for any mixture of pure nitride and pure oxide, which is taken here as an oxynitride where every Si atom is bounded to either oxygen or nitrogen atoms, but not with another Si. Each chemical reaction is ruled by one

reaction rate k_i , namely, k_1 and k_2 are related to NO and O₂ dissociation at the surface, k_3 , k_6 , k_7 , and k_9 concern the reactions between nonreacted silicon and the diffusive species (respectively, NO, O, O₂, and N). k_4 and k_8 govern the recombination of the atomic diffusive species producing O₂ or N₂. Finally, k_5 models the removal of N by diffusive O,¹³ a key ingredient to model the propagating nitrogen front that follows the oxynitride/Si interface. We also remark that fractional stoichiometric coefficients imply a mean-field approximation, since they describe the result of all possible reactions that transform the reactant species into the product ones. In this sense, coexistence at same depth x of fixed nitrogen, oxygen, and silicon in relative concentrations other than pure silicon, silicon nitride, or silicon oxide may be interpreted as silicon suboxides and/or subnitrides.

The origin of the two second partial derivatives on the right-hand sides of the first four equations is that jumping probabilities into regions containing partially nitrated (or oxidized) Si is modulated by the concentration of the nitrating species in these regions.¹⁴ The last equation, for ρ_{Si} , models the fact that whenever the network is oxidized or nitrated, some Si is released from the network, owing to volume differences of silicon atoms in bulk silicon and in silicon oxide or nitride.

Diffusion barriers in oxynitride films are accounted for by assuming diffusivities modulated by N local concentration: $D_i(x,t) = D_i^0 \exp(-c_i \rho_{\text{N}})$, where D_i^0 and c_i are constants, with $i = \text{O}, \text{O}_2$, or N. Thus, the higher the concentration of incorporated nitrogen, the smaller the diffusion coefficient for any diffusive species.¹⁴ The choice of an exponential function is based on two points: (i) It is a general function that, for adequate values of its parameters, is approximated by a linear function and (ii) as fixed nitrogen reduces diffusivity by blocking the passage of mobile species, we could assume that the incorporated nitrogen acts as a repulsive potential against the incoming particles. The average potential at a given depth x is expressed as a sum over all nitrogen atoms incorporated at that depth and hence the average potential is linearly dependent on the local concentration of fixed nitrogen atoms. However, usually diffusion coefficients depend exponentially on energy barriers. We have then chosen to describe diffusion coefficients to depend exponentially on local nitrogen concentrations.

The difficulty here is to deal with the estimation of so many reaction rates and diffusion coefficients. These parameters can, in principle, be determined experimentally, since each one is representing a different physical fact but we emphasize that the results are qualitatively robust against parameter variation inside adequate intervals, that is, keeping the same order of magnitude as the values we have chosen in what follows. The particular values of parameters values taken here are: $k_5 = 0.01$ (diffusive oxygen displacing fixed nitrogen), $k_8 = 1.0$ (two atomic nitrogen producing N₂), all other reaction rates are taken equal to 0.1. Furthermore, we take $D_{\text{O}}^0 = D_{\text{O}_2}^0 = D_{\text{N}}^0 = 0.1$; $c_{\text{O}} = c_{\text{O}_2} = c_{\text{N}} = 10$.

III. RESULTS AND DISCUSSION

The three oxynitride film growth routes are modeled, using the same reaction rates and diffusion functions: (i)

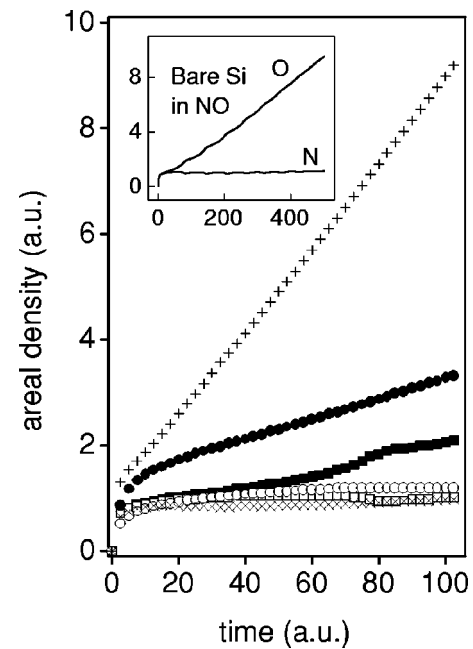


FIG. 2. N and O incorporation calculated curves, in arbitrary units (a.u.), for films grown on Si in NO (solid and empty squares) and N₂O (+ and ×) and for annealing of SiO₂ films on Si in NO (solid and empty circles). The inset presents N and O incorporation curves for Si in NO for longer times.

Thermal growth of oxynitride films on bare Si in NO, that is $P_{\text{NO}} = 0.1$, $P_{\text{O}_2} = 0.0$, $\rho_{\text{Si}}(x,t=0) = 1.0$, and other concentrations equal to zero for $x > 0$, (ii) thermal oxynitridation of SiO₂ films on Si in NO, that is $P_{\text{NO}} = 0.1$, $P_{\text{O}_2} = 0.0$, and $\rho_{\text{Si}}(x,t=0) = 0.44$, $\rho_{\text{O}}(x,t=0) = 0.88$, and other concentrations equal to zero for $0 < x < 10$, while $\rho_{\text{Si}}(x,t=0) = 1.0$ and other concentrations equal to zero for $x > 10$, and (iii) thermal growth of oxynitride films on Si in N₂O. Since it is well described in literature¹⁵ that N₂O promptly dissociates in the gas phase at high temperatures, giving NO and O₂ as end products, apart from inert N₂, this route can be emulated by growth of oxynitride films on bare Si in NO+O₂, that is $P_{\text{NO}} = 0.067$, $P_{\text{O}_2} = 0.033$, $\rho_{\text{Si}}(x,t=0) = 1.0$, and other concentrations equal to zero for $x > 0$. Figure 2 shows the model kinetics curves for incorporated O and N for the three routes as obtained by integration of the corresponding normalized densities.⁸ Bare Si in NO presents a plateau in the kinetics for incorporated O and N, which leads to a very slow, almost self-limited growth, up to 40 time units, when both species have been incorporated in comparable quantities. The kinetics curve asymptotically approaches a straight line after presenting damped oscillations (see inset of Fig. 2). These oscillations are a dynamical effect predicted by the model, reflecting the way the propagating N front finds its stationary state, and it remains to be determined whether or not this is observed in long time experiments. Oxynitridation of SiO₂ films in NO, leads to an approximately linear growth, except for the initial stages. Furthermore, oxynitride film growth on bare Si in NO+O₂ is rather faster. For the three growth routes, however, the amount of incorporated nitrogen is limited and stabilizes. The results of Fig. 2 compare qualitatively well with the experimental ones of Fig. 1.

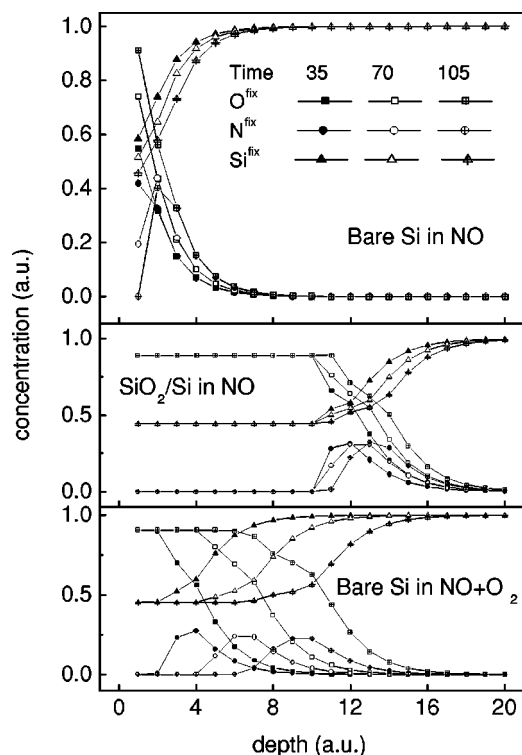


FIG. 3. Calculated density profiles, in a.u., of fixed species in silicon oxynitride films grown on Si in NO and N_2O and in annealing of SiO_2 films on Si in NO.

Figure 3 shows calculated density profiles for O, N, and Si resulting from growth of silicon oxynitride films in the three different routes discussed above, for different times. For bare Si in NO, early stages correspond to an oxygen plateau in the kinetics curves, due to the high concentration of incorporated nitrogen that slows down diffusion and therefore film growth. For these early stages, there are two different sources supplying N to the interface: Diffusing NO and atomic N, formed by NO dissociation at the surface. As atomic N is very reactive, it is responsible for the high N concentrations in the near-surface region. For longer times, however, atomic oxygen generated from NO dissociation at the surface, scavenges the incorporated nitrogen^{13,16} and a pure oxide film is formed on top of a reaction region composed of oxynitrides and nonfully reacted Si, localized at the near-interface region. As this front moves deeper into the sample, atomic nitrogen formed at the surface no longer contributes to N incorporation due to its fast recombination in near-surface regions. Consequently, the local N concentration near the interface is lower as compared to earlier stages, and mobile species diffusion to the moving reaction zone is enhanced. In fact, this is the explanation for the puzzling feature of oxide growth rates depending on the existence or not of initial silicon oxide films: These films effectively prevent atomic N, formed at the surface, from reaching the re-

active near-interface region. For longer times, when nitrogen accumulates at the interface leaving behind a pure silicon oxide film (this stage starts at approximately 40 time units, evidenced by the separation of incorporated N and O in the kinetics curves), incorporated N profiles tend to pile up in the near-interface region, as observed experimentally. Accordingly, the modeling of thermal oxynitridation in NO of SiO_2 films on Si does not present a plateau in the kinetics, since nitridation due only to the reaction of diffusive NO with substrate Si is not enough to create a major diffusion barrier to O_2 . One can see that N piles up in the near SiO_2 -Si interface in this case. The model profiles of Fig. 3 compare qualitatively well with the corresponding ones of Fig. 1. Finally, Fig. 3 shows model profiles at different times for growth on bare Si in N_2O (or $NO+O_2$) atmosphere. Oxygen is incorporated at a higher rate than in NO, but N incorporation repeats the reaction front picture, stabilizing at roughly the same values as for route 2. Competition between O_2 , NO, and atomic N channels prevents high N concentrations and the consequent formation of a plateau in the film growth kinetics. These model results also compare qualitatively well with the corresponding experimental facts given in Fig. 1.

In summary, the main qualitative features of experimental growth kinetics and N profiles in thermally grown silicon oxynitride films on Si presented here are well described by a reaction-diffusion model. Different growth routes are approached by changing only initial and boundary conditions, while keeping other parameters unchanged.

¹H. Z. Massoud, J. P. Shiely, and A. Shanware, *Mater. Res. Soc. Symp. Proc.* **567**, 227 (1999).

²A. Kingon, J.-P. Maria, and S. K. Streiffer, *Nature (London)* **406**, 1032 (2000).

³G. D. Wilk, R. M. Wallace, and J. M. Anthony, *J. Appl. Phys.* **89**, 5243 (2001).

⁴M. L. Green, E. P. Gusev, R. Degraeve, and E. L. Garfunkel, *J. Appl. Phys.* **90**, 2057 (2001).

⁵J. W. Kim, H. W. Yeom, K. J. Kong, B. D. Yu, D. Y. Ahn, Y. D. Chung, C. N. Whang, H. Yi, Y. H. Ha, and D. W. Moon, *Phys. Rev. Lett.* **90**, 106101 (2003).

⁶E. P. Gusev, H.-C. Lu, E. L. Garfunkel, T. Gustafsson, and M. L. Green, *IBM J. Res. Dev.* **43**, 265 (1999).

⁷A. Dasgupta and C. G. Takoudis, *J. Appl. Phys.* **93**, 3615 (2003).

⁸R. M. C. de Almeida, S. Gonçalves, I. J. R. Baumvol, and F. C. Stedile, *Phys. Rev. B* **61**, 12992 (2000).

⁹I. J. R. Baumvol, *Surf. Sci. Rep.* **36**, 1 (1999).

¹⁰H. C. Lu, E. P. Gusev, E. Garfunkel, B. W. Busch, T. Gustafsson, T. W. Sorsch, and M. L. Green, *J. Appl. Phys.* **87**, 1550 (2000); Z.-Q. Yao, *ibid.* **78**, 2906 (1995).

¹¹H. C. Lu, E. P. Gusev, T. Gustafsson, and E. Garfunkel, *J. Appl. Phys.* **81**, 6992 (1997).

¹²I. J. R. Baumvol, J.-J. Ganem, L. G. Gosset, I. Trimaille, and S. Rigo, *Appl. Phys. Lett.* **72**, 2999 (1998).

¹³E. C. Carr, K. A. Ellis, and R. A. Buhrman, *Appl. Phys. Lett.* **66**, 1492 (1995).

¹⁴R. M. C. de Almeida and I. J. R. Baumvol, *Phys. Rev. B* **62**, 16255 (2000).

¹⁵M. J. Hartig and P. J. Tobin, *J. Electrochem. Soc.* **143**, 1753 (1996).

¹⁶J. R. Baumvol, F. C. Stedile, J.-J. Ganem, I. Trimaille, and S. Rigo, *Appl. Phys. Lett.* **69**, 2385 (1996).